

Variational perturbation theory for density matrices

Michael Bachmann, Hagen Kleinert, and Axel Pelster

Institut für Theoretische Physik, Freie Universität Berlin, Arnimallee 14, 14195 Berlin, Germany

(Received 22 December 1998)

We develop a convergent variational perturbation theory for quantum-statistical density matrices which is applicable to polynomial as well as nonpolynomial interactions. We illustrate the power of the theory by calculating the temperature-dependent density of a particle in the double-well potential to second order, and of the electron in the hydrogen atom to first order. [S1050-2947(99)08410-3]

PACS number(s): 03.65.Ca, 05.30.-d

I. INTRODUCTION

Variational perturbation theory [1,2] transforms divergent perturbation expansions into convergent ones. The resulting convergence extends to infinitely strong couplings [3], a property which has recently been used to derive critical exponents in field theory without renormalization-group methods [4,5]. The theory was first developed in quantum mechanics for the path-integral representation of the free energy of the anharmonic oscillator [6] and the hydrogen atom [2,7]. Local quantities such as quantum-statistical density matrices have been treated so far only to lowest order for the anharmonic oscillator and the hydrogen atom [8,9]. Other rigorous nonperturbative approaches to compute the energy and the wave function of the ground state for quantum-mechanical systems were developed some time ago [10] and also more recently [11].

The purpose of this paper is to develop a systematic convergent variational perturbation theory for the path-integral representation of density matrices of a point particle moving in polynomial as well as nonpolynomial potentials. By systematically taking into account higher orders, we thus go beyond related first-order treatments in classical phase space [12] and early Rayleigh-Ritz-type variational approximations [13]. With the help of a generalized smearing formula which accounts for the effects of quantum fluctuations, we can furthermore treat nonpolynomial interactions, thus extending the range of applicability of the work in Ref. [14]. As a first application, here we calculate the particle density in the double-well potential to second order, and then the electron density in the hydrogen atom to first order.

II. GENERAL FEATURES

Variational perturbation theory approximates a quantum-statistical system by perturbation expansions around harmonic oscillators with trial frequencies which are optimized differently for each order of the expansions. When dealing with the free energy, it is essential to give a special treatment to the fluctuations of the path average $\bar{x} \equiv (k_B T/\hbar) \int_0^{\hbar/k_B T} d\tau x(\tau)$, since this performs violent fluctuations at high temperatures T . These cannot be treated by any expansion, unless the potential is close to harmonic. The effect of these fluctuations may, however, easily be calculated at the end by a single numerical fluctuation integral. For this reason, variational perturbation expansions are per-

formed for each position x_0 of the path average separately, yielding an N th-order approximation $W_N(x_0)$ to the local free energy $V_{\text{eff,cl}}(x_0)$, called the *effective classical potential* [15]. The name indicates that one may obtain the full quantum partition function Z from this object by a simple integral over x_0 just as in classical statistics,

$$Z = \int_{-\infty}^{+\infty} \frac{dx_0}{\sqrt{2\pi\hbar^2/Mk_B T}} e^{-V_{\text{eff,cl}}(x_0)/k_B T}. \quad (2.1)$$

Having calculated $W_N(x_0)$, we obtain the N th-order approximation to the partition function,

$$Z_N = \int_{-\infty}^{+\infty} \frac{dx_0}{\sqrt{2\pi\hbar^2/Mk_B T}} e^{-W_N(x_0)/k_B T}. \quad (2.2)$$

The separate treatment of the path average is important to ensure a fast convergence at larger temperatures. In the high-temperature limit, $W_N(x_0)$ converges against the initial potential $V(x_0)$ for any order N .

Before embarking upon the theory, it is useful to visualize some characteristic properties of path fluctuations. Consider the Euclidean path integral over all periodic paths $x(\tau)$, with $x(0) = x(\hbar/k_B T)$, for a harmonic oscillator with minimum at x_m , where the action is

$$\mathcal{A}_{\Omega, x_m}[x] = \int_0^{\hbar/k_B T} d\tau \left\{ \frac{1}{2} M \dot{x}^2(\tau) + \frac{1}{2} M \Omega^2 [x(\tau) - x_m]^2 \right\}. \quad (2.3)$$

Its partition function is

$$Z^{\Omega, x_m} = \oint \mathcal{D}x \exp\{-\mathcal{A}^{\Omega, x_m}[x]/\hbar\} = \frac{1}{2 \sinh \hbar \Omega / 2k_B T}, \quad (2.4)$$

and the correlation functions of local quantities $O_1(x), O_2(x), \dots$ are given by the expectation values

$$\begin{aligned} & \langle O_1(x(\tau_1)) O_2(x(\tau_2)) \cdots \rangle^{\Omega, x_m} \\ &= \frac{1}{Z^{\Omega, x_m}} \oint \mathcal{D}x O_1(x(\tau_1)) \\ & \quad \times O_2(x(\tau_2)) \cdots \exp\{-\mathcal{A}^{\Omega, x_m}[x]/\hbar\}. \end{aligned} \quad (2.5)$$

The particle distribution of the oscillator is given by

$$P_H(x) \equiv \langle \delta(x - x(\tau)) \rangle_{\Omega, x_m} = \frac{1}{\sqrt{2\pi a_H^2}} \exp\left[-\frac{(x - x_m)^2}{2a_H^2}\right], \quad (2.6)$$

which is a Gaussian distribution of width

$$a_H^2 = \frac{\hbar}{2M\Omega} \coth \frac{\hbar\Omega}{2k_B T}, \quad (2.7)$$

the subscript indicating that we are dealing with a harmonic oscillator. At zero temperature, this is equal to the square of the ground-state wave function of the harmonic oscillator, whose width is

$$a_{H0}^2 = \frac{\hbar}{2M\Omega}. \quad (2.8)$$

In the limit $\hbar \rightarrow 0$, from Eqs. (2.6) and (2.7) we obtain the classical distribution

$$P_{Hcl}(x) = \frac{1}{\sqrt{2\pi a_{Hcl}^2}} \exp\left[-\frac{(x - x_m)^2}{2a_{Hcl}^2}\right], \quad (2.9)$$

with

$$a_{Hcl}^2 = \frac{k_B T}{M\Omega^2}. \quad (2.10)$$

The linear growth of this classical width is the origin of the famous Dulong-Petit law for the specific heat of a harmonic system. The classical fluctuations are governed by the integral over the Boltzmann factor

$$e^{-M\Omega^2(x-x_m)^2/2k_B T} \quad (2.11)$$

in the classical partition function

$$Z_{Hcl} = \int_{-\infty}^{+\infty} \frac{dx}{\sqrt{2\pi\hbar^2/Mk_B T}} e^{-M\Omega^2(x-x_m)^2/2k_B T}. \quad (2.12)$$

From this we obtain the classical distribution (2.9) as the expectation value:

$$\begin{aligned} P_{Hcl}(x) &\equiv \langle \delta(x - \bar{x}) \rangle_{cl}^{\Omega, x_m} \\ &= Z_{cl}^{-1} \int_{-\infty}^{+\infty} \frac{d\bar{x}}{\sqrt{2\pi\hbar^2/Mk_B T}} \\ &\quad \times \delta(x - \bar{x}) e^{-M\Omega^2(\bar{x} - x_m)^2/2k_B T}. \end{aligned} \quad (2.13)$$

Variational perturbation theory avoids the divergence of the harmonic width a_H^2 at high temperatures in Eq. (2.10) by the separate treatment of the fluctuations of the path average \bar{x} , as explained above. The average is fixed at some value x_0 with the help of a delta function $\delta(\bar{x} - x_0)$. For each x_0 we introduce local expectation values

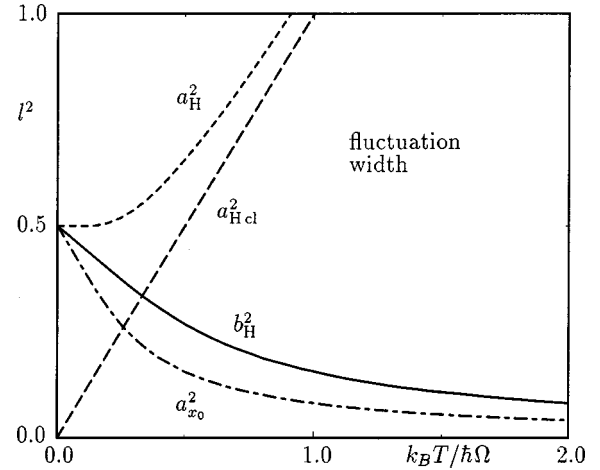


FIG. 1. Temperature dependence of fluctuation widths of any point $x(\tau)$ on the path in a harmonic oscillator (l^2 is a square length in units of $\hbar/M\Omega$). The quantity a_H^2 (dashed line) is the quantum-mechanical width, whereas $a_{x_0}^2$ (dash-dotted line) shares the width after separating out the fluctuations around the path average x_0 . The quantity a_{Hcl}^2 (long-dashed line) is the width of the classical distribution, and b_H^2 (solid curve) is the fluctuation width at fixed ends which is relevant for the calculation of the density matrix by variational perturbation theory (see Sec. III).

$$\begin{aligned} &\langle O_1(x(\tau_1)) O_2(x(\tau_2)) \cdots \rangle_{x_0}^{\Omega, x_m} \\ &= \frac{\langle \delta(\bar{x} - x_0) O_1(x(\tau_1)) O_2(x(\tau_2)) \cdots \rangle_{x_0}^{\Omega, x_m}}{\langle \delta(\bar{x} - x_0) \rangle_{x_0}^{\Omega, x_m}}. \end{aligned} \quad (2.14)$$

The original quantum statistical distribution of the harmonic oscillator (2.6) collects fluctuations of $\bar{x} = x_0$ and those around x_0 , and can therefore be written as a convolution

$$P_H(x) = \int_{-\infty}^{+\infty} dx_0 P_{x_0}(x - x_0) P_{Hcl}(x_0), \quad (2.15)$$

over the classical distribution (2.9) and the local one

$$P_{x_0}(x) = \langle \delta(x - x(\tau)) \rangle_{x_0}^{\Omega, x_m} = \frac{1}{\sqrt{2\pi a_{x_0}^2}} \exp\left[-\frac{(x - x_0)^2}{2a_{x_0}^2}\right]. \quad (2.16)$$

Such a convolution of Gaussian distributions as in Eq. (2.15) leads to another Gaussian distribution with added widths, so that the width of the local distribution is given by the difference

$$a_{x_0}^2 = a_{Hcl}^2 - a_{cl}^2 = \frac{\hbar}{2M\Omega} \left(\coth \frac{\hbar\Omega}{2k_B T} - \frac{2k_B T}{\hbar\Omega} \right), \quad (2.17)$$

which starts out at the finite value (2.8) for $T=0$, and goes to zero for $T \rightarrow \infty$ with the asymptotic behavior $\hbar\Omega/12k_B T$ (see Fig. 1). The latter property suppresses all fluctuations around \bar{x} and guarantees that $\lim_{T \rightarrow \infty} W_N(x_0) = V(x_0)$ for all N .

With this separation of the path average, the partition function

$$Z = \oint Dx \exp\{-\mathcal{A}[x]/\hbar\} \quad (2.18)$$

for the general particle action

$$\mathcal{A}[x] = \int_0^{\hbar/k_B T} d\tau \left[\frac{1}{2} M \dot{x}^2(\tau) + V(x(\tau)) \right] \quad (2.19)$$

possesses the effective classical representation (2.1) with the effective classical potential

$$V_{\text{eff,cl}}(x_0) = -k_B T \ln \left[\left(\frac{2\pi\hbar^2}{Mk_B T} \right)^{1/2} \oint \mathcal{D}x \delta(x_0 - \bar{x}) \times \exp\{-\mathcal{A}[x]/\hbar\} \right]. \quad (2.20)$$

In variational perturbation theory [2], this is expanded perturbatively around an x_0 -dependent harmonic system with trial frequency $\Omega(x_0)$, whose optimization leads to the approximation $W_N(x_0)$ for $V_{\text{eff,cl}}(x_0)$.

III. DENSITY MATRIX OF HARMONIC OSCILLATOR

In the present paper we dwell on the question how this method can be extended to the density matrix

$$\rho(x_b, x_a) = \frac{1}{Z} \tilde{\rho}(x_b, x_a), \quad (3.1)$$

where $\tilde{\rho}(x_b, x_a)$ is the path integral,

$$\tilde{\rho}(x_b, x_a) = \int_{(x_a, 0) \rightsquigarrow (x_b, \hbar/k_B T)} \mathcal{D}x \exp\{-\mathcal{A}[x]/\hbar\}, \quad (3.2)$$

over all paths with the fixed end points $x(0) = x_a$ and $x(\hbar/k_B T) = x_b$. The partition function is found from the trace of $\tilde{\rho}(x_b, x_a)$:

$$Z = \int_{-\infty}^{+\infty} dx \tilde{\rho}(x, x). \quad (3.3)$$

For a harmonic oscillator centered at x_m with the action (2.3), the path integral (3.2) can be easily done with the result (see Chap. 2 in Ref. [2])

$$\begin{aligned} \tilde{\rho}_0^{\Omega, x_m}(x_b, x_a) &= \left(\frac{M\Omega}{2\pi\hbar \sinh \hbar\Omega/k_B T} \right)^{1/2} \\ &\times \exp \left\{ -\frac{M\Omega}{2\hbar \sinh \hbar\Omega/k_B T} \right. \\ &\left. \times [(\tilde{x}_b^2 + \tilde{x}_a^2) \cosh \hbar\Omega/k_B T - 2\tilde{x}_b \tilde{x}_a] \right\}, \end{aligned} \quad (3.4)$$

where we introduced the abbreviation

$$\tilde{x}(\tau) = x(\tau) - x_m. \quad (3.5)$$

At fixed end points x_b, x_a , the quantum-mechanical correlation functions are

$$\langle O_1(x(\tau_1)) O_2(x(\tau_2)) \cdots \rangle_{x_b, x_a}^{\Omega, x_m} = \frac{1}{\tilde{\rho}_0^{\Omega, x_m}(x_b, x_a)} \int_{(x_a, 0) \rightsquigarrow (x_b, \hbar/k_B T)} \mathcal{D}x O_1(x(\tau_1)) O_2(x(\tau_2)) \cdots \exp\{-\mathcal{A}^{\Omega, x_m}[x]/\hbar\}, \quad (3.6)$$

and the distribution function is given by

$$\begin{aligned} p_H(x, \tau) &\equiv \langle \delta(x - x(\tau)) \rangle_{x_b, x_a}^{\Omega, x_m} \\ &= \frac{1}{\sqrt{2\pi b_H^2(\tau)}} \exp \left[-\frac{(\tilde{x} - x_{\text{cl}}(\tau))^2}{2b_H^2(\tau)} \right]. \end{aligned} \quad (3.7)$$

The classical path of a particle in a harmonic potential is

$$x_{\text{cl}}(\tau) = \frac{\tilde{x}_b \sinh \Omega \tau + \tilde{x}_a \sinh \Omega(\hbar/k_B T - \tau)}{\sinh \hbar\Omega/k_B T} \quad (3.8)$$

and the time-dependent width $b_H^2(\tau)$ is found to be

$$b_H^2(\tau) = \frac{\hbar}{2M\Omega} \left\{ \coth \frac{\hbar\Omega}{k_B T} - \frac{\cosh[\Omega(2\tau - \hbar/k_B T)]}{\sinh \hbar\Omega/k_B T} \right\}. \quad (3.9)$$

Since the Euclidean time τ lies in the interval $0 \leq \tau \leq \hbar/k_B T$, the width (3.9) is bounded by

$$b_H^2(\tau) \leq \frac{\hbar}{2M\Omega} \tanh \frac{\hbar\Omega}{2k_B T}, \quad (3.10)$$

thus remaining finite at all temperatures. The temporal average of Eq. (3.9) is

$$b_H^2 = \frac{k_B T}{\hbar} \int_0^{\hbar/k_B T} d\tau b_H^2(\tau) = \frac{\hbar}{2M\Omega} \left(\coth \frac{\hbar\Omega}{k_B T} - \frac{k_B T}{\hbar\Omega} \right). \quad (3.11)$$

Just as $a_{x_0}^2$, this goes to zero for $T \rightarrow \infty$ with an asymptotic behavior $\hbar\Omega/6k_B T$, which is twice as large as that of $a_{x_0}^2$ (see Fig. 1).

IV. VARIATIONAL PERTURBATION THEORY FOR DENSITY MATRICES

To obtain a variational approximation for the density matrix, it is useful to separate the general action (2.19) into a trial one for which the Euclidean propagator is known, and a remainder containing the original potential. If we were to

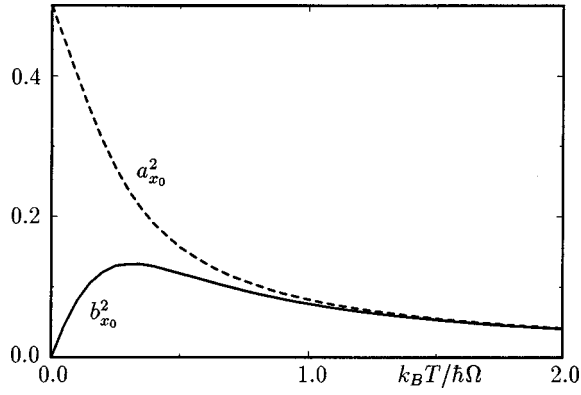


FIG. 2. Temperature dependence of the width of fluctuations around the path average $x_0 = \bar{x}$ at fixed ends. For comparison we also show the width $a_{x_0}^2$ of Fig. 1. The vertical axis gives these square lengths l^2 in units of $\hbar/M\Omega$ again.

proceed in complete analogy with the treatment of the partition function, we would expand the Euclidean path integral around a trial harmonic one with fixed end points x_b and x_a and a fixed path average x_0 , and with a trial frequency $\Omega(x_b, x_a; x_0)$. The result would be an effective classical potential $W_N(x_b, x_a; x_0)$ to be optimized in $\Omega(x_b, x_a; x_0)$. After that we would have to perform a final integral in x_0 over the Boltzmann factor $\exp[-W_N(x_b, x_a; x_0)/k_B T]$.

However, because of the finiteness of the fluctuation width b_H^2 at all temperatures which is similar to that of $a_{x_0}^2$, the special treatment of $\bar{x} = x_0$ becomes superfluous for paths with fixed end points x_b, x_a . While the separation of x_0 was necessary to deal with the diverging fluctuation width of the path average \bar{x} , paths with fixed ends have fluctuations of the path average which are governed by the distribution

$$\begin{aligned} p_{x_0}(x_b, x_a) &\equiv \langle \delta(x_0 - \bar{x}) \rangle_{x_b, x_a}^{\Omega, x_m} \\ &= \frac{1}{\sqrt{2\pi b_{x_0}^2}} \exp \left\{ -\frac{1}{2b_{x_0}^2} \left[\bar{x}_0 \right. \right. \\ &\quad \left. \left. - \frac{1}{2}(\bar{x}_b + \bar{x}_a) \frac{2k_B T}{\hbar \Omega} \tanh \frac{\hbar \Omega}{2k_B T} \right]^2 \right\} \quad (4.1) \end{aligned}$$

with the width

$$b_{x_0}^2 = \frac{k_B T}{M\Omega^2} \left[1 - \frac{2k_B T}{\hbar \Omega} \tanh \frac{\hbar \Omega}{2k_B T} \right], \quad (4.2)$$

which goes to zero for both limits $T \rightarrow 0$ and $T \rightarrow \infty$ (see Fig. 2). At each Euclidean time, $x(\tau)$ fluctuates narrowly around the classical path $x_{cl}(\tau)$ connecting x_b and x_a . This is the reason why we may treat the fluctuations of $\bar{x} = x_0$ by variational perturbation theory, just as the other fluctuations. As a remnant of the extra treatment of x_0 we must, however, perform the initial perturbation expansion around the minimum of the effective classical potential which will lie at some point x_m determined by the end points x_b and x_a and by the minimum of the potential $V(x)$. Thus we shall use the Euclidean path integral for the density matrix of the harmonic oscillator centered at x_m as the trial system around which to

perform the variational perturbation theory, treating the fluctuations of x_0 around x_m on the same footing as the remaining fluctuations. The position x_m of the minimum is a function $x_m = x_m(x_b, x_a)$, and has to be optimized with respect to the trial frequency, which itself is a function $\Omega = \Omega(x_b, x_a)$ to be optimized.

Hence we start by decomposing action (2.19) as

$$\mathcal{A}[x] = \mathcal{A}^{\Omega, x_m}[x] + \mathcal{A}_{\text{int}}[x], \quad (4.3)$$

with an interaction

$$\mathcal{A}_{\text{int}}[x] = \int_0^{\hbar\beta} d\tau V_{\text{int}}(x(\tau)), \quad (4.4)$$

where the interaction potential is the difference between the original one $V(x)$ and the inserted displaced harmonic oscillator:

$$V_{\text{int}}(x) = V(x) - \frac{1}{2} M \Omega^2 [x - x_m]^2. \quad (4.5)$$

For brevity, we have introduced the inverse temperature in natural units $\beta \equiv 1/k_B T$ in Eq. (4.4). Now we evaluate the path integral for the Euclidean propagator (3.2) by treating the interaction (4.4) as a perturbation, leading to a moment expansion

$$\begin{aligned} \tilde{\rho}(x_b, x_a) &= \tilde{\rho}_0^{\Omega, x_m}(x_b, x_a) \left[1 - \frac{1}{\hbar} \langle \mathcal{A}_{\text{int}}[x] \rangle_{x_b, x_a}^{\Omega, x_m} \right. \\ &\quad \left. + \frac{1}{2\hbar^2} \langle \mathcal{A}_{\text{int}}^2[x] \rangle_{x_b, x_a}^{\Omega, x_m} - \dots \right], \quad (4.6) \end{aligned}$$

with expectation values defined in Eq. (3.6). The zeroth order consists of the harmonic contribution (3.4) and higher orders contain harmonic averages of the interaction (4.4). The correlation functions in Eq. (4.6) can be decomposed into connected ones by going over to cumulants, yielding

$$\begin{aligned} \tilde{\rho}(x_b, x_a) &= \tilde{\rho}_0^{\Omega, x_m}(x_b, x_a) \exp \left[-\frac{1}{\hbar} \langle \mathcal{A}_{\text{int}}[x] \rangle_{x_b, x_a, c}^{\Omega, x_m} \right. \\ &\quad \left. + \frac{1}{2\hbar^2} \langle \mathcal{A}_{\text{int}}^2[x] \rangle_{x_b, x_a, c}^{\Omega, x_m} - \dots \right], \quad (4.7) \end{aligned}$$

where the first cumulants are defined as usual

$$\begin{aligned} \langle O_1(x(\tau_1)) \rangle_{x_b, x_a, c}^{\Omega, x_m} &= \langle O_1(x(\tau_1)) \rangle_{x_b, x_a}^{\Omega, x_m}, \\ \langle O_1(x(\tau_1)) O_2(x(\tau_2)) \rangle_{x_b, x_a, c}^{\Omega, x_m} &= \langle O_1(x(\tau_1)) O_2(x(\tau_2)) \rangle_{x_b, x_a}^{\Omega, x_m} \\ &\quad - \langle O_1(x(\tau_1)) \rangle_{x_b, x_a}^{\Omega, x_m} \langle O_2(x(\tau_2)) \rangle_{x_b, x_a}^{\Omega, x_m}. \end{aligned} \quad (4.8)$$

Series (4.7) is truncated after the N th term, resulting in the N th-order approximant for the quantum-statistical density matrix

$$\begin{aligned} \tilde{\rho}_N^{\Omega, x_m}(x_b, x_a) &= \tilde{\rho}_0^{\Omega, x_m}(x_b, x_a) \\ &\times \exp \left[\sum_{n=1}^N \frac{(-1)^n}{n! \hbar^n} \langle \mathcal{A}_{\text{int}}^n[x] \rangle_{x_b, x_a, c}^{\Omega, x_m} \right], \end{aligned} \quad (4.9)$$

which explicitly depends on both variational parameters Ω and x_m .

In analogy to classical statistics, where the Boltzmann distribution in configuration space is controlled by the classical potential $V(x)$ according to

$$\tilde{\rho}_{\text{cl}}(x) = \left(\frac{M}{2\pi\hbar^2\beta} \right)^{1/2} \exp[-\beta V(x)], \quad (4.10)$$

we now introduce an *effective classical potential* $V_{\text{eff,cl}}(x_b, x_a)$ which governs the unnormalized density matrix

$$\tilde{\rho}(x_b, x_a) = \left(\frac{M}{2\pi\hbar^2\beta} \right)^{1/2} \exp[-\beta V_{\text{eff,cl}}(x_b, x_a)]. \quad (4.11)$$

Its N th-order approximation is obtained from Eqs. (3.4), (4.9), and (4.11) via the cumulant expansion

$$\begin{aligned} W_N^{\Omega, x_m}(x_b, x_a) &= \frac{1}{2\beta} \ln \frac{\sinh \hbar \beta \Omega}{\hbar \beta \Omega} \\ &+ \frac{M\Omega}{2\hbar\beta \sinh \hbar \beta \Omega} \\ &\times \{ (\tilde{x}_b^2 + \tilde{x}_a^2) \cosh \hbar \beta \Omega - 2\tilde{x}_b \tilde{x}_a \} \\ &- \frac{1}{\beta} \sum_{n=1}^N \frac{(-1)^n}{n! \hbar^n} \langle \mathcal{A}_{\text{int}}^n[x] \rangle_{x_b, x_a, c}^{\Omega, x_m}, \end{aligned} \quad (4.12)$$

which is optimized for each set of end points x_b and x_a in the variational parameters Ω^2 and x_m , the result being denoted by $W_N(x_b, x_a)$. The optimal values $\Omega^2(x_b, x_a)$ and $x_m(x_b, x_a)$ are determined from the extremality conditions

$$\frac{\partial W_N^{\Omega, x_m}(x_b, x_a)}{\partial \Omega^2} = 0, \quad \frac{\partial W_N^{\Omega, x_m}(x_b, x_a)}{\partial x_m} = 0. \quad (4.13)$$

The solutions are denoted by Ω^{2N} and x_m^N , both being functions of x_b and x_a . If no extrema are found, one has to look for the flattest region of function (4.12), where the lowest higher-order derivative disappears. Eventually the N th-order approximation for the normalized density matrix is obtained from

$$\rho_N(x_b, x_a) = Z_N^{-1} \tilde{\rho}_N^{\Omega^{2N}, x_m^N}(x_b, x_a), \quad (4.14)$$

where the corresponding partition function reads

$$Z_N = \int_{-\infty}^{+\infty} dx \tilde{\rho}_N^{\Omega^{2N}, x_m^N}(x_b, x_a). \quad (4.15)$$

In principle, one could also optimize the entire ratio (4.14), but this would be harder to do in practice. Moreover, the optimization of the unnormalized density matrix is the only option, if the normalization diverges due to singularities of the potential. This will be seen in Sec. VIII B by the example of the hydrogen atom.

V. SMEARING FORMULA FOR DENSITY MATRICES

In order to calculate the connected correlation functions in the variational perturbation expansion (4.9), we must find efficient formulas for evaluating expectation values (3.6) of any power of the interaction (4.4):

$$\begin{aligned} \langle \mathcal{A}_{\text{int}}^n[x] \rangle_{x_b, x_a}^{\Omega, x_m} &= \frac{1}{\tilde{\rho}_0^{\Omega, x_m}(x_b, x_a)} \int_{\tilde{x}_a, 0}^{\tilde{x}_b, \hbar\beta} \mathcal{D}\tilde{x} \\ &\times \prod_{l=1}^n \left[\int_0^{\hbar\beta} d\tau_l V_{\text{int}}(\tilde{x}(\tau_l) + x_m) \right] \\ &\times \exp \left\{ -\frac{1}{\hbar} \mathcal{A}^{\Omega, x_m}[\tilde{x} + x_m] \right\}. \end{aligned} \quad (5.1)$$

This can be done by an extension of the smearing formalism which is developed in Ref. [7]. To this end we rewrite the interaction potential as

$$\begin{aligned} V_{\text{int}}(\tilde{x}(\tau_l) + x_m) &= \int_{-\infty}^{+\infty} dz_l V_{\text{int}}(z_l + x_m) \\ &\times \int_{-\infty}^{+\infty} \frac{d\lambda_l}{2\pi} \exp\{i\lambda_l z_l\} \\ &\times \exp \left[-\int_0^{\hbar\beta} d\tau i\lambda_l \delta(\tau - \tau_l) \tilde{x}(\tau) \right], \end{aligned} \quad (5.2)$$

and introduce a current

$$J(\tau) = \sum_{l=1}^n i\hbar \lambda_l \delta(\tau - \tau_l), \quad (5.3)$$

so that Eq. (5.1) becomes

$$\begin{aligned} \langle \mathcal{A}_{\text{int}}^n[x] \rangle_{x_b, x_a}^{\Omega, x_m} &= \frac{1}{\tilde{\rho}_0^{\Omega, x_m}(x_b, x_a)} \prod_{l=1}^n \left[\int_0^{\hbar\beta} d\tau_l \right. \\ &\times \int_{-\infty}^{+\infty} dz_l V_{\text{int}}(z_l + x_m) \\ &\times \left. \int_{-\infty}^{+\infty} \frac{d\lambda_l}{2\pi} \exp\{i\lambda_l z_l\} \right] K^{\Omega, x_m}[J]. \end{aligned} \quad (5.4)$$

The kernel $K^{\Omega, x_m}[J]$ represents the generating functional for all correlation functions of the displaced harmonic oscillator

$$K^{\Omega, x_m}[J] = \int_{\bar{x}_a, 0}^{\bar{x}_b, \hbar\beta} \mathcal{D}\bar{x} \exp \left\{ -\frac{1}{\hbar} \int_0^{\hbar\beta} d\tau \left[\frac{m}{2} \dot{\bar{x}}^2(\tau) + \frac{1}{2} M \Omega^2 \bar{x}^2(\tau) + J(\tau) \bar{x}(\tau) \right] \right\}. \quad (5.5)$$

For zero current J , this generating functional reduces to the Euclidean harmonic propagator (3.4):

$$K^{\Omega, x_m}[J=0] = \tilde{\rho}_0^{\Omega, x_m}(x_b, x_a). \quad (5.6)$$

For nonzero J , the solution of the functional integral (5.5) is given by (see Chap. 3 in Ref. [2])

$$K^{\Omega, x_m}[J] = \tilde{\rho}_0^{\Omega, x_m}(x_b, x_a) \exp \left[-\frac{1}{\hbar} \int_0^{\hbar\beta} d\tau J(\tau) x_{\text{cl}}(\tau) + \frac{1}{2\hbar^2} \int_0^{\hbar\beta} d\tau \int_0^{\hbar\beta} d\tau' J(\tau) G^{\Omega}(\tau, \tau') J(\tau') \right], \quad (5.7)$$

where $x_{\text{cl}}(\tau)$ denotes the classical path (3.8) and $G^{\Omega}(\tau, \tau')$ the harmonic Green function

$$G^{\Omega}(\tau, \tau') = \frac{\hbar}{2M\Omega} \times \frac{\cosh \Omega(|\tau - \tau'| - \hbar\beta) - \cosh \Omega(\tau + \tau' - \hbar\beta)}{\sinh \hbar\beta\Omega}. \quad (5.8)$$

Expression (5.7) can be simplified by using the explicit expression (5.3) for the current J . This leads to a generating functional

$$K^{\Omega, x_m}[J] = \tilde{\rho}_0^{\Omega, x_m}(x_b, x_a) \exp(-i\boldsymbol{\lambda}^T \mathbf{x}_{\text{cl}} - \frac{1}{2} \boldsymbol{\lambda}^T G \boldsymbol{\lambda}), \quad (5.9)$$

where we have introduced the n -dimensional vectors $\boldsymbol{\lambda} = (\lambda_1, \dots, \lambda_n)^T$ and $\mathbf{x}_{\text{cl}} = (x_{\text{cl}}(\tau_1), \dots, x_{\text{cl}}(\tau_n))^T$, with the superscript T denoting transposition, and the symmetric $n \times n$ matrix G whose elements are $G_{kl} = G^{\Omega}(\tau_k, \tau_l)$. Inserting Eq. (5.9) into Eq. (5.4), and performing the integrals with respect to $\lambda_1, \dots, \lambda_n$, we obtain the n th-order smearing formula for the density matrix

$$\langle \mathcal{A}_{\text{int}}^n[x] \rangle_{x_b, x_a}^{\Omega, x_m} = \prod_{l=1}^n \left[\int_0^{\hbar\beta} d\tau_l \int_{-\infty}^{+\infty} dz_l V_{\text{int}}(z_l + x_m) \right] \frac{1}{\sqrt{(2\pi)^n \det G}} \exp \left\{ -\frac{1}{2} \sum_{k,l=1}^n [z_k - x_{\text{cl}}(\tau_k)] G_{kl}^{-1} [z_l - x_{\text{cl}}(\tau_l)] \right\}. \quad (5.10)$$

The integrand contains an n -dimensional Gaussian distribution describing both thermal and quantum fluctuations around the harmonic classical path $x_{\text{cl}}(\tau)$ of Eq. (3.8) in a trial oscillator centered at x_m , whose width is governed by the Green function (5.8).

For closed paths with coinciding end points ($x_b = x_a$), formula (5.10) leads to the n th-order smearing formula for particle densities,

$$\rho(x_a) = \frac{1}{Z} \tilde{\rho}(x_a, x_a) = \frac{1}{Z} \oint \mathcal{D}x \delta(x(\tau=0) - x_a) \exp\{-A[x]/\hbar\}, \quad (5.11)$$

which can be written as

$$\langle \mathcal{A}_{\text{int}}^n[x] \rangle_{x_a, x_a}^{\Omega, x_m} = \frac{1}{\rho_0^{\Omega, x_m}(x_a)} \times \prod_{l=1}^n \left[\int_0^{\hbar\beta} d\tau_l \int_{-\infty}^{+\infty} dz_l V_{\text{int}}(z_l + x_m) \right] \times \frac{1}{\sqrt{(2\pi)^{n+1} \det a^2}} \exp \left(-\frac{1}{2} \sum_{k,l=0}^n z_k a_{kl}^{-2} z_l \right), \quad (5.12)$$

with $z_0 = \bar{x}_a$ and $\tau_0 = 0$. Here a^2 denotes a symmetric $(n+1) \times (n+1)$ matrix whose elements $a_{kl}^2 = a^2(\tau_k, \tau_l)$ are obtained from the harmonic Green function for periodic paths $G^{\Omega, p}(\tau, \tau')$ as (see Chaps. 3 and 5 in Ref. [2])

$$a^2(\tau, \tau') \equiv \frac{\hbar}{M} G^{\Omega, p}(\tau, \tau') = \frac{\hbar}{2M\Omega} \frac{\cosh \Omega(|\tau - \tau'| - \hbar\beta/2)}{\sinh \hbar\beta\Omega/2}. \quad (5.13)$$

The diagonal elements $a^2 = a^2(\tau, \tau)$ represent the fluctuation width (2.7), which behaves in the classical limit like Eq. (2.10) and at zero temperature like Eq. (2.8).

Both smearing formulas (5.10) and (5.12) allow one in principle to determine all harmonic expectation values for the variational perturbation theory of density matrices and particle densities in terms of ordinary Gaussian integrals. Unfortunately, in many applications containing nonpolynomial potentials, it is impossible to solve either the spatial or the temporal integrals analytically. This circumstance drastically increases the numerical effort in higher-order calculations.

VI. FIRST-ORDER VARIATIONAL RESULTS

The first-order variational approximation usually gives a reasonable estimate for any desired quantity. Let us investigate the classical and quantum-mechanical limit of this approximation. To facilitate the discussion, we first derive an alternative representation for the first-order smearing formula

(5.12) which allows a direct evaluation of the imaginary-time integral. The resulting expression will depend only on temperature, whose low- and high-temperature limits can easily be extracted.

A. Alternative formula for first-order smearing

For simplicity, we restrict ourselves to the case of particle densities, and allow only symmetric potentials $V(x)$ centered at the origin. If $V(x)$ has only one minimum at the origin, then x_m will also be zero. If $V(x)$ has several symmetric minima, then x_m goes to zero only at sufficiently high temperatures (see Chap. 5 in Ref. [2]).

To first order, the smearing formula (5.12) reads

$$\langle \mathcal{A}_{\text{int}}[x] \rangle_{x_a, x_a}^{\Omega} = \frac{1}{\rho_0^{\Omega}(x_a)} \int_0^{\hbar\beta} d\tau \int_{-\infty}^{+\infty} \frac{dz}{2\pi} V_{\text{int}}(z) \frac{1}{\sqrt{a_{00}^4 - a_{01}^4}} \times \exp\left\{-\frac{1}{2} \frac{(z^2 + x_a^2)a_{00}^2 - 2zx_a a_{01}^2}{a_{00}^4 - a_{01}^4}\right\}, \quad (6.1)$$

so that Mehler's summation formula

$$\frac{1}{\sqrt{1-b^2}} \exp\left\{-\frac{(x^2+x'^2)(1+b^2)-4xx'b}{2(1-b^2)}\right\} = \exp\left\{-\frac{1}{2}(x^2+x'^2)\right\} \sum_{n=0}^{\infty} \frac{b^n}{2^n n!} H_n(x) H_n(x') \quad (6.2)$$

leads to an expansion in terms of Hermite polynomials $H_n(x)$, whose temperature dependence stems from the diagonal elements of the harmonic Green function (5.13):

$$\langle \mathcal{A}_{\text{int}}[x] \rangle_{x_a, x_a}^{\Omega} = \sum_{n=0}^{\infty} \frac{\hbar\beta}{2^n n!} C_{\beta}^{(n)} H_n(x_a/\sqrt{2a_{00}^2}) \times \int_{-\infty}^{+\infty} \frac{dz}{\sqrt{2\pi a_{00}^2}} V_{\text{int}}(z) e^{-z^2/2a_{00}^2} H_n(z/\sqrt{2a_{00}^2}). \quad (6.3)$$

Here the dimensionless functions $C_{\beta}^{(n)}$ are defined by

$$C_{\beta}^{(n)} = \frac{1}{\hbar\beta} \int_0^{\hbar\beta} d\tau \left(\frac{a_{01}^2}{a_{00}^2}\right)^n \quad (6.4)$$

and their temperature dependence is shown in Fig. 3). Inserting Eq. (5.13) and performing the integral over τ , we obtain

$$C_{\beta}^{(n)} = \frac{1}{2^n \cosh^n \hbar\beta\Omega/2} \sum_{k=0}^n \binom{n}{k} \frac{\sinh \hbar\beta\Omega(n/2-k)}{\hbar\beta\Omega(n/2-k)}. \quad (6.5)$$

At high temperatures, these functions of β go all to unity,

$$\lim_{\beta \rightarrow 0} C_{\beta}^{(n)} = 1, \quad (6.6)$$

whereas for zero temperature we yield

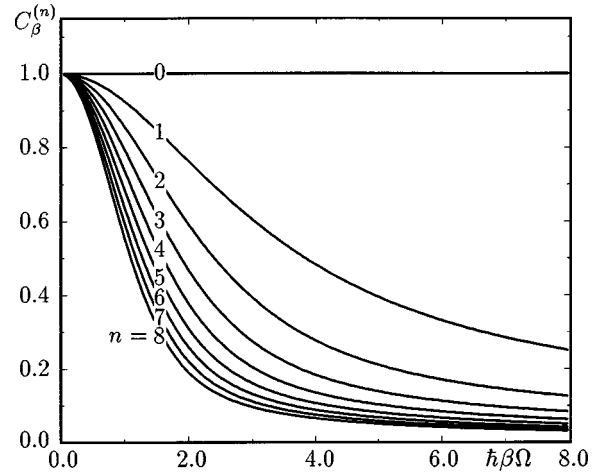


FIG. 3. Temperature dependence of the first nine functions $C_{\beta}^{(n)}$, where $\beta=1/k_B T$.

$$\lim_{\beta \rightarrow \infty} C_{\beta}^{(n)} = \begin{cases} 1, & n=0 \\ \frac{2}{\hbar\beta\Omega n}, & n>0. \end{cases} \quad (6.7)$$

According to Eq. (4.12), the first-order approximation to the effective classical potential is given by

$$W_1^{\Omega}(x_a) = \frac{1}{2\beta} \ln \frac{\sinh \hbar\beta\Omega}{\hbar\beta\Omega} + \frac{M\Omega}{\hbar\beta} x_a^2 \tanh \frac{\hbar\beta\Omega}{2} + V_{a_2}^{\Omega}(x_a), \quad (6.8)$$

with the smeared interaction potential

$$V_{a_2}^{\Omega}(x_a) = \frac{1}{\hbar\beta} \langle \mathcal{A}_{\text{int}}[x] \rangle_{x_a, x_a}^{\Omega}. \quad (6.9)$$

It is instructive to discuss separately the limits $\beta \rightarrow 0$ and $\beta \rightarrow \infty$ of dominating thermal and quantum fluctuations, respectively.

B. Classical limit of effective classical potential

In the classical limit $\beta \rightarrow 0$, the first-order effective classical potential (6.8) reduces to

$$W_1^{\Omega, \text{cl}}(x_a) = \frac{1}{2} M\Omega^2 x_a^2 + \lim_{\beta \rightarrow 0} V_{a_2}^{\Omega}(x_a). \quad (6.10)$$

The second term is determined by inserting the high-temperature limit of the fluctuation width (2.10) and of the polynomials (6.6) into expansion (6.3), leading to

$$\lim_{\beta \rightarrow 0} V_{a_2}^{\Omega}(x_a) = \lim_{\beta \rightarrow 0} \sum_{n=0}^{\infty} \frac{1}{2^n n!} H_n(\sqrt{M\Omega^2\beta/2} x_a) \times \int_{-\infty}^{+\infty} \frac{dz}{\sqrt{2\pi/M\Omega^2\beta}} V_{\text{int}}(z) e^{-M\Omega^2\beta z^2/2} \times H_n(\sqrt{M\Omega^2\beta/2} z). \quad (6.11)$$

Then we make use of the completeness relation for Hermite polynomials,

$$\frac{1}{\sqrt{\pi}} e^{-x^2} \sum_{n=0}^{\infty} \frac{1}{2^n n!} H_n(x) H_n(x') = \delta(x-x'), \quad (6.12)$$

which may be derived from Mehler's summation formula (6.2) in the limit $b \rightarrow 1^-$, to reduce the smeared interaction potential $V_{a^2}^{\Omega}(x_a)$ to the pure interaction potential (4.5):

$$\lim_{\beta \rightarrow 0} V_{a^2}^{\Omega}(x_a) = V_{\text{int}}(x_a). \quad (6.13)$$

Recalling Eq. (4.5) we see that the first-order effective classical potential (6.10) approaches the classical one:

$$\lim_{\beta \rightarrow 0} W_1^{\Omega, \text{cl}}(x_a) = V(x_a). \quad (6.14)$$

This is a consequence of the vanishing fluctuation width b_H^2 of the paths around the classical orbits. This property is universal to all higher-order approximations to the effective classical potential (4.12). Thus all correction terms with $n > 1$ must disappear in the limit $\beta \rightarrow 0$:

$$\lim_{\beta \rightarrow 0} \frac{-1}{\beta} \sum_{n=2}^{\infty} \frac{(-1)^n}{n! \hbar^n} \langle \mathcal{A}_{\text{int}}^n[x] \rangle_{x_a, x_a, c}^{\Omega} = 0. \quad (6.15)$$

C. Zero-temperature limit

At low temperatures, the first-order effective classical potential (6.8) becomes

$$W_1^{\Omega, \text{qm}}(x_a) = \frac{\hbar \Omega}{2} + \lim_{\beta \rightarrow \infty} V_{a^2}^{\Omega}(x_a). \quad (6.16)$$

The zero-temperature limit of the smeared potential in the second term defined in Eq. (6.9) follows from Eq. (6.3) by taking into account the limiting procedure for the polynomials $C_{\beta}^{(n)}$ in Eq. (6.7) and for the fluctuation width (2.8). Thus with $H_0(x) = 1$ and the inverse length $\kappa = \sqrt{M\Omega/\hbar}$ we obtain

$$\lim_{\beta \rightarrow \infty} V_{a^2}^{\Omega}(x_a) = \int_{-\infty}^{+\infty} dz \left(\frac{\kappa^2}{\pi} \right)^{1/2} H_0(\kappa z)^2 \times \exp\{-\kappa^2 z^2\} V_{\text{int}}(z). \quad (6.17)$$

Introducing the harmonic eigenvalues

$$E_n^{\Omega} = \hbar \Omega \left(n + \frac{1}{2} \right), \quad (6.18)$$

and the harmonic eigenfunctions

$$\psi_n^{\Omega}(x) = \frac{1}{\sqrt{n! 2^n}} \left(\frac{\kappa^2}{\pi} \right)^{1/4} e^{-\kappa^2 x^2/2} H_n(\kappa x), \quad (6.19)$$

we can reexpress the zero-temperature limit of the first-order effective classical potential (6.16) with Eq. (6.17) by

$$W_1^{\Omega, \text{qm}}(x_a) = E_0^{\Omega} + \langle \psi_0^{\Omega} | V_{\text{int}} | \psi_0^{\Omega} \rangle. \quad (6.20)$$

This is recognized as the first-order harmonic Rayleigh-Schrödinger perturbative result for the ground-state energy.

For the discussion of the quantum-mechanical limit of the first-order normalized density,

$$\rho_1^{\Omega}(x_a) = \frac{\tilde{\rho}_1^{\Omega}(x_a)}{Z}$$

$$= \rho_0^{\Omega}(x_a) \frac{\exp\left\{-\frac{1}{\hbar} \langle \mathcal{A}_{\text{int}}[x] \rangle_{x_a, x_a}^{\Omega}\right\}}{\int_{-\infty}^{+\infty} dx_a \rho_0^{\Omega}(x_a) \exp\left\{-\frac{1}{\hbar} \langle \mathcal{A}_{\text{int}}[x] \rangle_{x_a, x_a}^{\Omega}\right\}}, \quad (6.21)$$

we proceed as follows. First we expand Eq. (6.21) up to first order in the interaction, leading to

$$\rho_1^{\Omega}(x_a) = \rho_0^{\Omega}(x_a) \left[1 - \frac{1}{\hbar} \left(\langle \mathcal{A}_{\text{int}}[x] \rangle_{x_a, x_a}^{\Omega} - \int_{-\infty}^{+\infty} dx_a \rho_0^{\Omega}(x_a) \times \langle \mathcal{A}_{\text{int}}[x] \rangle_{x_a, x_a}^{\Omega} \right) \right]. \quad (6.22)$$

Inserting Eqs. (3.4) and (6.3) into the third term in Eq. (6.22), and assuming Ω not to depend explicitly on x_a , the x_a integral reduces to the orthonormality relation for Hermite polynomials

$$\frac{1}{2^n n! \sqrt{\pi}} \int_{-\infty}^{+\infty} dx_a H_n(x_a) H_0(x_a) e^{-x_a^2} = \delta_{n0}, \quad (6.23)$$

so that the third term in Eq. (6.22) eventually becomes

$$- \int_{-\infty}^{+\infty} dx_a \rho_0^{\Omega}(x_a) \langle \mathcal{A}_{\text{int}}[x] \rangle_{x_a, x_a}^{\Omega} = -\beta \int_{-\infty}^{+\infty} dz \left(\frac{\kappa^2}{\pi} \right)^{1/2} V_{\text{int}}(z) \exp\{-\kappa^2 z^2\} H_0(\kappa z). \quad (6.24)$$

But this is just the $n=0$ term of Eq. (6.3) with an opposite sign, thus cancelling the zeroth component of the second term in Eq. (6.22), which would have been divergent for $\beta \rightarrow \infty$.

The resulting expression for the first-order normalized density is

$$\rho_1^{\Omega}(x_a) = \rho_0^{\Omega}(x_a) \times \left[1 - \sum_{n=1}^{\infty} \frac{\beta}{2^n n!} C_{\beta}^{(n)} H_n(\kappa x_a) \times \int_{-\infty}^{+\infty} dz \left(\frac{\kappa^2}{\pi} \right)^{1/2} V_{\text{int}}(z) \exp(-\kappa^2 z^2) H_n(\kappa z) \right]. \quad (6.25)$$

The zero-temperature limit of $C_{\beta}^{(n)}$ is, from Eqs. (6.7) and (6.18),

$$\lim_{\beta \rightarrow \infty} \beta C_{\beta}^{(n)} = \frac{2}{E_n^{\Omega} - E_0^{\Omega}}, \quad (6.26)$$

so that from Eq. (6.25) we obtain the limit

$$\begin{aligned} \rho_1^{\Omega}(x_a) &= \rho_0^{\Omega}(x_a) \\ &\times \left[1 - 2 \sum_{n=1}^{\infty} \frac{1}{2^n n!} \frac{1}{E_n^{\Omega} - E_0^{\Omega}} H_n(\kappa x_a) \right. \\ &\times \int_{-\infty}^{+\infty} dz \left(\frac{\kappa^2}{\pi} \right)^{1/2} V_{\text{int}}(z) \\ &\left. \times \exp\{-\kappa^2 z^2\} H_n(\kappa z) H_0(\kappa z) \right]. \quad (6.27) \end{aligned}$$

Taking into account the harmonic eigenfunctions (6.19), we can rewrite Eq. (6.27) as

$$\begin{aligned} \rho_1^{\Omega}(x_a) &= |\psi_0(x_a)|^2 \\ &= [\psi_0^{\Omega}(x_a)]^2 - 2 \psi_0^{\Omega}(x_a) \sum_{n>0} \psi_n^{\Omega}(x_a) \frac{\langle \psi_n^{\Omega} | V_{\text{int}} | \psi_0^{\Omega} \rangle}{E_n^{\Omega} - E_0^{\Omega}}, \quad (6.28) \end{aligned}$$

which is just equivalent to the harmonic first-order Rayleigh-Schrödinger result for particle densities.

Summarizing the results of this section, we have shown that our method has properly reproduced the high- and low-temperature limits. Because of relation (6.28), the variational approach for particle densities can be used to determine the ground-state wave function $\psi_0(x_a)$ approximately for the system of interest.

More recently an independent variational approach has been proposed [11]. Another rigorous, fully nonperturbative way to compute the energy and the wave function of the ground state for quantum-mechanical systems was developed by generalizing the WKB method to more than one dimension [10].

VII. SMEARING FORMULA IN HIGHER SPATIAL DIMENSIONS

Most physical systems possess many degrees of freedom. This requires an extension of our method to higher spatial dimensions. In general, we must consider anisotropic harmonic trial systems, where the previous variational parameter Ω^2 becomes a $D \times D$ matrix $\Omega_{\mu\nu}^2$, with $\mu, \nu = 1, 2, \dots, D$.

A. Isotropic approximation

An isotropic trial ansatz

$$\Omega_{\mu\nu}^2 = \Omega^2 \delta_{\mu\nu} \quad (7.1)$$

can give rough initial estimates for the properties of the system. In this case, the n th-order smearing formula (5.12) generalizes directly to

$$\begin{aligned} \langle \mathcal{A}_{\text{int}}^n[r] \rangle_{\mathbf{r}_a, \mathbf{r}_a}^{\Omega} &= \frac{1}{\rho_0^{\Omega}(\mathbf{r}_a)} \prod_{l=1}^n \left[\int_0^{\hbar\beta} d\tau_l \int d^D z_l V_{\text{int}}(\mathbf{z}_l) \right] \\ &\times \frac{1}{\sqrt{(2\pi)^{n+1} \det a^{2D}}} \\ &\times \exp \left[-\frac{1}{2} \sum_{k,l=0}^n \mathbf{z}_k a_{kl}^{-2} \mathbf{z}_l \right], \quad (7.2) \end{aligned}$$

with the D -dimensional vectors $\mathbf{z}_l = (z_{1l}, z_{2l}, \dots, z_{Dl})^T$. Note, that Greek labels $\mu, \nu, \dots = 1, 2, \dots, D$ specify spatial indices, and Latin labels $k, l, \dots = 0, 1, 2, \dots, n$ refer to the different imaginary times. The vector \mathbf{z}_0 denotes \mathbf{r}_a , and the matrix a^2 is the same as in Sec. V. The harmonic density reads

$$\rho_0^{\Omega}(\mathbf{r}) = \left(\frac{1}{2\pi a_{00}^2} \right)^{D/2} \exp \left[-\frac{1}{2a_{00}^2} \sum_{\mu=1}^D x_{\mu}^2 \right]. \quad (7.3)$$

B. Anisotropic approximation

In the discussion of the anisotropic approximation, we shall only consider radially symmetric potentials $V(\mathbf{r}) = V(|\mathbf{r}|)$ because of their simplicity and their major occurrence in physics. The trial frequencies decompose naturally into a radial frequency Ω_L and a transversal one Ω_T (see Ref. [2]):

$$\Omega_{\mu\nu}^2 = \Omega_L^2 \frac{x_{a\mu} x_{a\nu}}{r_a^2} + \Omega_T^2 \left(\delta_{\mu\nu} - \frac{x_{a\mu} x_{a\nu}}{r_a^2} \right), \quad (7.4)$$

with $r_a = |\mathbf{r}_a|$. For practical reasons we rotate the coordinate system by $\bar{\mathbf{x}}_n = U \mathbf{x}_n$ so that $\bar{\mathbf{r}}_a$ points along the first coordinate axis,

$$(\bar{\mathbf{r}}_a)_{\mu} \equiv \bar{z}_{\mu 0} = \begin{cases} r_a, & \mu = 1 \\ 0, & 2 \leq \mu \leq D, \end{cases} \quad (7.5)$$

and the rotated Ω^2 matrix is diagonal:

$$\bar{\Omega}^2 = \begin{pmatrix} \Omega_L^2 & 0 & 0 & \cdots & 0 \\ 0 & \Omega_T^2 & 0 & \cdots & 0 \\ 0 & 0 & \Omega_T^2 & \cdots & 0 \\ \vdots & \vdots & \vdots & \ddots & \vdots \\ 0 & 0 & 0 & \cdots & \Omega_T^2 \end{pmatrix} = U \Omega^2 U^{-1}. \quad (7.6)$$

After this rotation, the *anisotropic* n th-order smearing formula in D dimensions reads

$$\begin{aligned} \langle \mathcal{A}_{\text{int}}^n[\mathbf{r}] \rangle_{\mathbf{r}_a, \mathbf{r}_a}^{\Omega_L, T} &= \frac{1}{\rho_0^{\Omega_L, T}(\bar{\mathbf{r}}_a)} \prod_{l=1}^n \left[\int_0^{\hbar\beta} d\tau_l \int d^D \bar{z}_l V_{\text{int}}(|\bar{\mathbf{z}}_l|) \right] (2\pi)^{-D(n+1)/2} (\det a_L^2)^{-1/2} (\det a_T^2)^{-(D-1)/2} \\ &\times \exp \left\{ -\frac{1}{2} \sum_{k,l=0}^n \bar{z}_{1k} a_{Lkl}^{-2} \bar{z}_{1l} \right\} \exp \left\{ -\frac{1}{2} \sum_{\mu=2}^D \sum_{k,l=1}^n \bar{z}_{\mu k} a_{Tkl}^{-2} \bar{z}_{\mu l} \right\}. \end{aligned} \quad (7.7)$$

The components of the longitudinal and transversal matrices a_L^2 and a_T^2 are

$$a_{Lkl}^2 = a_L^2(\tau_k, \tau_l), \quad a_{Tkl}^2 = a_T^2(\tau_k, \tau_l), \quad (7.8)$$

where the frequency Ω in Eq. (5.13) must be substituted for the variational parameters Ω_L and Ω_T , respectively. For the harmonic density in the rotated system $\rho_0^{\Omega_L, T}(\bar{\mathbf{r}})$ which is used to normalize Eq. (7.7), we find

$$\begin{aligned} \rho_0^{\Omega_L, T}(\bar{\mathbf{r}}) &= \left(\frac{1}{2\pi a_{L00}^2} \right)^{1/2} \left(\frac{1}{2\pi a_{T00}^2} \right)^{D-1/2} \\ &\times \exp \left[-\frac{1}{2a_{L00}^2} \bar{x}_1^2 - \frac{1}{2a_{T00}^2} \sum_{\mu=2}^D \bar{x}_\mu^2 \right]. \end{aligned} \quad (7.9)$$

VIII. APPLICATIONS

By discussing the applications, we shall employ for simplicity natural units with $\hbar = k_B = M = 1$. In order to develop some feeling about how our variational method works, we first approximate the particle density in the double-well potential in second order. After that we approximate the temperature-dependent electron density of the hydrogen atom in first order.

A. Double well

A detailed analysis of the first-order approximation shows that the particle density in the double-well potential is nearly exact for all temperatures if we use the two variational parameters Ω^2 and x_m , whereas one variational parameter Ω^2 leads to larger deviations at low temperatures and coupling strengths. For such conditions, leading to a maximum of density far away from the origin, $x_a = 0$, the displacement of the trial oscillator x_m may not be supposed to vanish. Considering this, our first-order results improve those obtained in Ref. [14]. Since the differences between the optimization procedures using one or two variational parameters become less significant in higher orders, the subsequent second-order calculation is restricted to the optimization in Ω .

1. First-order approximation

In the case of the double-well potential

$$V(x) = -\frac{1}{2} \omega^2 x^2 + \frac{1}{4} g x^4 + \frac{1}{4g} \quad (8.1)$$

with coupling constant g , we obtain for the expectation of the interaction (6.3) to first order, also setting $\omega^2 = 1$,

$$\begin{aligned} \langle \mathcal{A}[x] \rangle_{x_a, x_a}^{\Omega, x_m} &= \frac{1}{2} \beta g_0 + \frac{1}{2} g_1 C_\beta^{(1)} H_1((x_a - x_m)/\sqrt{2a_{00}^2}) \\ &+ \frac{1}{4} g_2 C_\beta^{(2)} H_2((x_a - x_m)/\sqrt{2a_{00}^2}) \\ &+ \frac{1}{8} g_3 C_\beta^{(3)} H_3((x_a - x_m)/\sqrt{2a_{00}^2}) \\ &+ \frac{1}{16} g_4 C_\beta^{(4)} H_4((x_a - x_m)/\sqrt{2a_{00}^2}), \end{aligned} \quad (8.2)$$

with

$$\begin{aligned} g_0 &= -a_{00}^2(\Omega^2 + 1) + \frac{3}{2} g a_{00}^4 + 3g a_{00}^2 x_m^2 + \frac{1}{2} g x_m^4 \\ &+ \frac{1}{2g} - \frac{1}{2} x_m^2, \\ g_1 &= -\sqrt{2a_{00}^2} x_m + \frac{3}{4} g (2a_{00}^2)^{3/2} x_m + g \sqrt{2a_{00}^2} x_m^3, \\ g_2 &= -a_{00}^2(\Omega^2 + 1) + 3g a_{00}^4 + 3g a_{00}^2 x_m^2, \\ g_3 &= g (2a_{00}^2)^{3/2} x_m, \\ g_4 &= g a_{00}^4. \end{aligned}$$

Inserting Eq. (8.2) into Eq. (6.9) and using Eq. (6.8), we obtain the unnormalized double-well density

$$\bar{\rho}_1^{\Omega, x_m}(x_a) = \frac{1}{\sqrt{2\pi\beta}} \exp[-\beta W_1^{\Omega, x_m}(x_a)], \quad (8.3)$$

with the first-order effective classical potential

$$\begin{aligned} W_1^{\Omega, x_m}(x_a) &= \frac{1}{2} \ln \frac{\sinh \beta\Omega}{\beta\Omega} + \frac{\Omega}{\beta} (x_a - x_m)^2 \tanh \frac{\beta\Omega}{2} \\ &+ \frac{1}{\beta} \langle \mathcal{A}_{\text{int}}[x] \rangle_{x_a, x_a}^{\Omega, x_m}. \end{aligned} \quad (8.4)$$

After optimizing $W_1^{\Omega, x_m}(x_a)$, the normalized first-order particle density $\rho_1(x_a)$ is found by dividing $\bar{\rho}_1(x_a)$ by the first-order partition function

$$Z_1 = \frac{1}{\sqrt{2\pi\beta}} \int_{-\infty}^{+\infty} dx_a \exp[-\beta W_1(x_a)]. \quad (8.5)$$

Subjecting $W_1^{\Omega, x_m}(x_a)$ to the extremality conditions (4.13), we obtain optimal values for the variational parameters $\Omega^2(x_a)$ and $x_m(x_a)$. Usually there is a unique minimum, but sometimes this does not exist and a turning point or a vanishing higher derivative must be used for optimization. For-

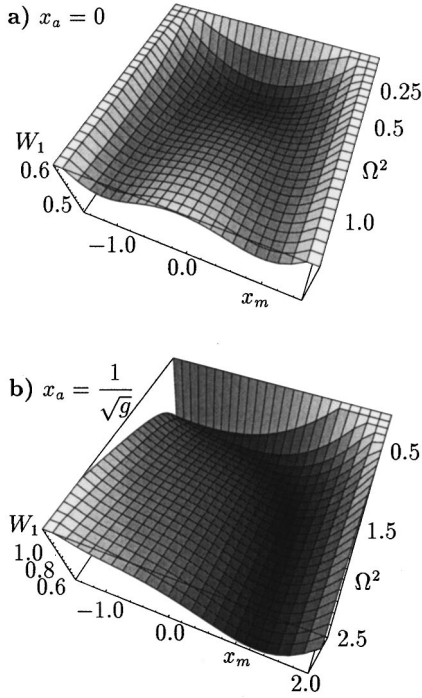


FIG. 4. Plots of the first-order approximation $W_1^{\Omega, x_m}(x_a)$ to the effective classical potential as a function of the two variational parameters $\Omega^2(x_a)$ and $x_m(x_a)$ at $g=0.4$ and $\beta=10$ for two different values of x_a .

tunately, the first case is often realized. Figure 4 shows the dependence of the first-order effective classical potential $W_1^{\Omega, x_m}(x_a)$ at $\beta=10$ and $g=0.4$ for two fixed values of position x_a as a function of the variational parameters $\Omega^2(x_a)$ and $x_m(x_a)$ in a three-dimensional plot. Thereby, the darker the region the smaller the value of W_1^{Ω, x_m} . We can distinguish between deep valleys (dark gray), in which the global minimum resides, and hills (light gray). After having roughly determined the area around the expected minimum, one numerically solves the extremality conditions (4.13) with some nearby starting values, to find the exact locations of the minimum. The example in Fig. 4 gives an impression of the general features of this minimization process. Furthermore we note that, for symmetry reasons,

$$x_m(x_a) = -x_m(-x_a), \quad (8.6)$$

and

$$\Omega^2(x_a) = \Omega^2(-x_a). \quad (8.7)$$

Some first-order approximations of the effective classical potential $W_1(x_a)$ are shown in Fig. 5, which are obtained by optimizing with respect to $\Omega^2(x_a)$ and $x_m(x_a)$. The sharp maximum occurring for weak coupling is a consequence of a nonvanishing $x_m(x_a=0)$. In the strong-coupling regime, on the other hand, where $x_m(x_a=0) \approx 0$, the sharp top is absent. This behavior is illustrated in Figs. 6(b) and 7(b) at different temperatures. In Fig. 6(b) we see that for $x_a > 0$, the optimal x_m values lie close to the right-hand minimum of the double-well potential, which we only want to consider here. The minimum is located at $1/\sqrt{g} \approx 3.16$.

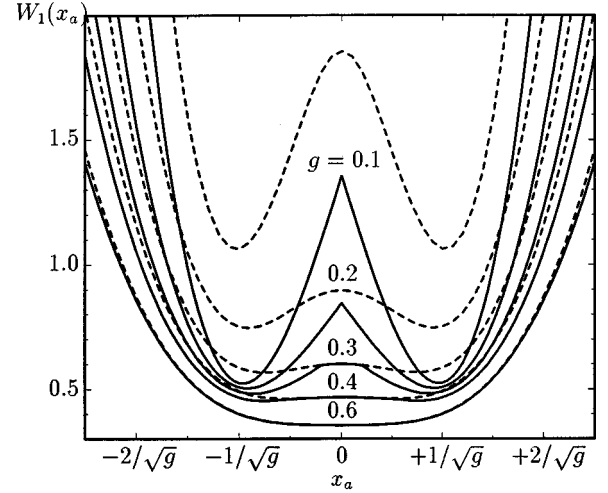


FIG. 5. First-order approximation of the effective classical potential, $W_1(x_a)$, for different coupling strengths g as a function of the position x_a at $\beta=10$ by optimizing in both variational parameters Ω^2 and x_m (solid curves) in comparison with the approximations obtained by variation in Ω^2 only (dashed curves).

The influence of the center parameter x_m diminishes for increasing values of g and decreasing height $1/4g$ of the central barrier (see Fig. 5). The same thing is true at high temperatures and large values of x_a , where the precise knowledge of the optimal value of x_m is irrelevant. In these limits, the particle density can be determined without optimizing in x_m , simply setting $x_m=0$, where the expectation value Eq. (8.2) reduces to

$$\begin{aligned} \langle \mathcal{A}_{\text{int}}[x] \rangle_{x_a, x_a}^{\Omega} &= \frac{1}{4} C_{\beta}^{(2)} H_2(x_a / \sqrt{2a_{00}^2}) (g_1 + 3g_2) \\ &\quad + \frac{1}{16} g_2 C_{\beta}^{(4)} H_4(x_a / \sqrt{2a_{00}^2}) \\ &\quad + \beta \left(\frac{1}{2} g_1 + \frac{3}{4} g_2 + g_3 \right), \end{aligned} \quad (8.8)$$

with the abbreviations

$$g_1 = -a_{00}^2(\Omega^2 + 1), \quad g_2 = g a_{00}^4, \quad g_3 = \frac{1}{4g}.$$

Inserting Eq. (8.8) into Eq. (6.9) and using Eq. (6.8), we obtain the unnormalized double-well density

$$\tilde{\rho}_1^{\Omega}(x_a) = \frac{1}{\sqrt{2\pi\beta}} \exp[-\beta W_1^{\Omega}(x_a)], \quad (8.9)$$

with the first-order effective classical potential

$$W_1^{\Omega}(x_a) = \frac{1}{2} \ln \frac{\sinh \beta \Omega}{\beta \Omega} + \frac{\Omega}{\beta} x_a^2 \tanh \frac{\beta \Omega}{2} + \frac{1}{\beta} \langle \mathcal{A}_{\text{int}}[x] \rangle_{x_a, x_a}^{\Omega}. \quad (8.10)$$

The optimization at $x_m=0$ gives reasonable results for moderate temperatures at couplings such as $g=0.4$, as shown in Fig. 8 by a comparison with the exact density which is obtained from numerical solution of the Schrödinger equation. An additional optimization in x_m cannot be distinguished on the plot. An example where the second variational parameter x_m becomes important is shown in Fig. 9, where we compare

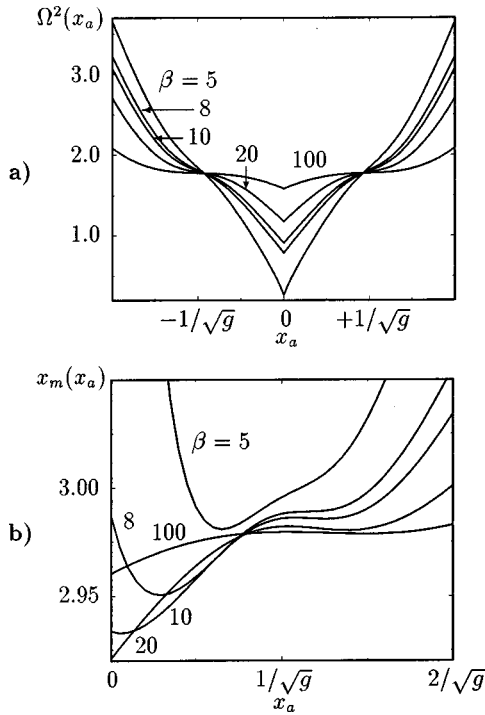


FIG. 6. (a) Trial frequency $\Omega^2(x_a)$ at different temperatures and coupling strength $g=0.1$. (b) Minimum of the trial oscillator $x_m(x_a)$ at different temperatures and coupling strength $g=0.1$.

the first-order approximation with one (Ω) and two variational parameters (Ω, x_m) with the exact density for different temperatures at the smaller coupling strength $g=0.1$. We observe that, with two variational parameters, the first-order approximation is nearly exact for all temperatures, in contrast to the results with only one variational parameter at low temperatures (see the curve for $\beta=20$).

2. Second-order approximation

In second-order variational perturbation theory, the differences between the optimization procedures using one or two variational parameters become less significant. Thus we restrict ourselves to the optimization in $\Omega(x_a)$, and set $x_m=0$.

The second-order density

$$\tilde{\rho}_2^\Omega(x_a) = \frac{1}{\sqrt{2\pi\beta}} \exp[-\beta W_2^\Omega(x_a)] \quad (8.11)$$

with the second-order approximation of the effective classical potential

$$W_2^\Omega(x_a) = \frac{1}{2} \ln \frac{\sinh \beta\Omega}{\beta\Omega} + \frac{\Omega}{\beta} x_a^2 \tanh \frac{\beta\Omega}{2} + \frac{1}{\beta} \langle \mathcal{A}_{\text{int}}[x] \rangle_{x_a, x_a}^\Omega - \frac{1}{2\beta} \langle \mathcal{A}_{\text{int}}^2[x] \rangle_{x_a, x_a}^\Omega \quad (8.12)$$

requires evaluating the smearing formula (5.10) for $n=1$, which is given in Eq. (8.8), and $n=2$ to be calculated. Going immediately to the cumulant we have

$$\begin{aligned} \langle \mathcal{A}_{\text{int}}^2[x] \rangle_{x_a, x_a, c}^\Omega &= \int_0^{\hbar\beta} d\tau_1 \int_0^{\hbar\beta} d\tau_2 \left\{ \frac{1}{4} (\Omega^2 + 1)^2 [I_{22}(\tau_1, \tau_2) \right. \\ &\quad - I_2(\tau_1)I_2(\tau_2)] - \frac{1}{4} g (\Omega^2 + 1) [I_{24}(\tau_1, \tau_2) \\ &\quad - I_2(\tau_1)I_4(\tau_2)] + \frac{1}{16} g^2 [I_{44}(\tau_1, \tau_2) \\ &\quad \left. - I_4(\tau_1)I_4(\tau_2)] \right\}, \quad (8.13) \end{aligned}$$

with

$$I_m(\tau_k) = (a_{00}^4 - a_{0k}^4)^m \frac{\partial^m}{\partial j^m} \exp \left[\frac{j^2 + 2x_a a_{0k}^2 j}{2a_{00}^2 (a_{00}^4 - a_{0k}^4)} \right]_{j=0}, \quad k=1,2 \quad (8.14)$$

and

$$\begin{aligned} I_{mn}(\tau_1, \tau_2) &= (-\det A)^{m+n} \frac{\partial^m}{\partial j_1^m} \frac{\partial^n}{\partial j_2^n} \exp \left[\frac{F(j_1, j_2)}{2a_{00}^2 (\det A)^2} \right]_{j_1=j_2=0} \\ \det A &= a_{00}^6 + 2a_{01}^2 a_{02}^2 a_{12}^2 - a_{00}^2 (a_{01}^4 + a_{02}^4 + a_{12}^4). \quad (8.15) \end{aligned}$$

The generating function is

$$\begin{aligned} F(j_1, j_2) &= a_{00}^4 (j_1^2 + j_2^2) - 2a_{00}^6 (a_{01}^2 j_1 + a_{02}^2 j_2) x_a \\ &\quad + 2a_{00}^2 (a_{12}^2 j_1 j_2 + (a_{01}^4 + a_{02}^4 + a_{12}^4) (a_{01}^2 j_1 \\ &\quad + a_{02}^2 j_2) x_a) - (a_{01}^2 j_1 + a_{02}^2 j_2) (a_{01}^2 j_1 + a_{02}^2 j_2 \\ &\quad + 4a_{01}^2 a_{02}^2 a_{12}^2 x_a). \quad (8.16) \end{aligned}$$

All necessary derivatives and the imaginary time integrations in Eq. (8.13) have been calculated analytically. After optimizing the unnormalized second-order density (8.11) in Ω , we obtain the results depicted in Fig. 10. Comparing the second-order results with the exact densities obtained from numerical solutions of the Schrödinger equation, we see that the deviations are strongest in the region of intermediate β , as expected. Quantum-mechanical limits are reproduced very well, classical limits exactly.

B. Distribution function for the electron in the hydrogen atom

With the insights gained in Sec. VIII A by discussing the double-well potential, we are prepared to apply our method to the electron in the hydrogen atom which is exposed to the attractive Coulomb interaction

$$V(\mathbf{r}) = -\frac{e^2}{r}. \quad (8.17)$$

Apart from its physical significance, the theoretical interest in this problem originates from the nonpolynomial nature of the attractive Coulomb interaction. The usual Wick rules or Feynman diagrams do not allow one to evaluate harmonic expectation values in this case. Only by the aid of the above-mentioned smearing formula are we able to compute the

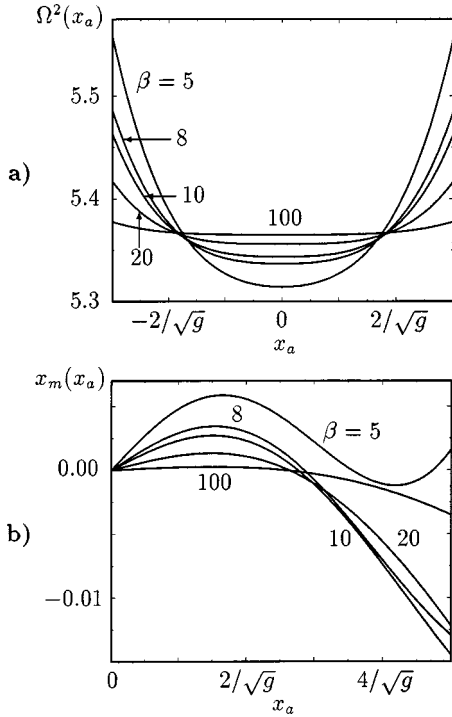


FIG. 7. (a) Trial frequency $\Omega^2(x_a)$ at different temperatures and coupling strength $g = 10$. (b) Minimum of trial oscillator $x_m(x_a)$ at different temperatures and coupling strength $g = 10$.

variational expansion. Since we learned from the double-well potential that the importance of the second variational parameter \mathbf{r}_m diminishes for a decreasing height of the central barrier, it is sufficient for the Coulomb potential with an absent central barrier to set $\mathbf{r}_m = 0$ and to take into account only one variational parameter Ω^2 . By doing so we will see in first order that the anisotropic variational approximation becomes significant at low temperatures, where radial and transversal quantum fluctuations have quite different weights. The effect of anisotropy disappears completely in the classical limit.

1. Isotropic first-order approximation

In the first-order approximation for the unnormalized density, we must calculate the harmonic expectation value of the action,

$$\mathcal{A}_{\text{int}}[r] = \int_0^{\hbar\beta} d\tau_1 V_{\text{int}}(\mathbf{r}(\tau_1)), \quad (8.18)$$

with the interaction potential

$$V_{\text{int}}(\mathbf{r}) = -\left(\frac{e^2}{r} + \frac{1}{2} \mathbf{r}^T \Omega^2 \mathbf{r}\right), \quad (8.19)$$

where the matrix $\Omega_{\mu\nu}^2$ has the form of Eq. (7.4). Applying the isotropic smearing formula (7.2) for $n=1$ to the harmonic term in Eq. (8.18), we easily find

$$\langle \mathbf{r}^2(\tau_1) \rangle_{\mathbf{r}_a, r_a}^{\Omega} = 3 \frac{a_{00}^4 - a_{01}^4}{a_{00}^2} + \frac{a_{01}^4}{a_{00}^4} r_a^2. \quad (8.20)$$

For the Coulomb potential we obtain the local average

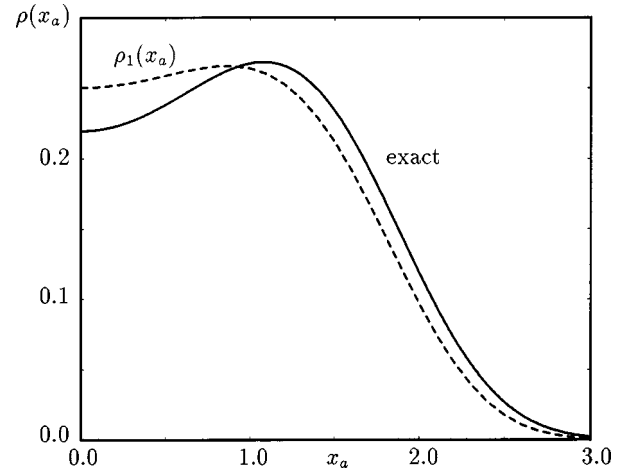


FIG. 8. First-order approximation of the double-well particle density for $\beta = 10$ and $g = 0.4$ compared with the exact particle density from numerical solution of the Schrödinger equation. All values are in natural units.

$$\left\langle \frac{e^2}{r(\tau_1)} \right\rangle_{\mathbf{r}_a, r_a}^{\Omega} = \frac{e^2}{r_a} \frac{a_{00}^2}{a_{01}^2} \operatorname{erf}\left(\frac{a_{01}^2}{\sqrt{2a_{00}^2(a_{00}^4 - a_{01}^4)}} r_a\right). \quad (8.21)$$

The time integration in Eq. (8.18) cannot be done in an analytical manner and must be performed numerically. Alternatively we can use the expansion method introduced in Sec. VIA for evaluating the smearing formula in three dimensions, which yields

$$\begin{aligned} \langle \mathcal{A}_{\text{int}}[\mathbf{r}] \rangle_{\mathbf{r}_a, r_a}^{\Omega} &= [\rho_0^{\Omega}(\mathbf{r}_a)]^{-1} \frac{e^{-r_a^2/2a_{00}^2}}{\pi^2 a_{00}^2 r_a} \\ &\times \sum_{n=0}^{\infty} \frac{H_{2n+1}(r_a/\sqrt{2a_{00}^2})}{2^{2n+1}(2n+1)!} C_{\beta}^{(2n)} \\ &\times \int_0^{\infty} dy y V_{\text{int}}(\sqrt{2a_{00}^2} y) e^{-y^2} H_{2n+1}(y). \end{aligned} \quad (8.22)$$

This can be rewritten in terms of Laguerre polynomials $L_n^{\mu}(r)$ as

$$\begin{aligned} \langle \mathcal{A}_{\text{int}}[\mathbf{r}] \rangle_{\mathbf{r}_a, r_a}^{\Omega} &= \left(\frac{2a_{00}^2}{\pi}\right)^{1/2} \frac{1}{r_a} \sum_{n=0}^{\infty} \frac{(-1)^n n!}{(2n+1)!} C_{\beta}^{(2n)} \\ &\times H_{2n+1}(r_a/\sqrt{2a_{00}^2}) \int_0^{\infty} dy y^{1/2} \\ &\times V_{\text{int}}(\sqrt{2a_{00}^2} y^{1/2}) e^{-y} L_n^{1/2}(y) L_0^{1/2}(y). \end{aligned} \quad (8.23)$$

Using the integral formula [Ref. [16], Eq. (2.19.14.15)],

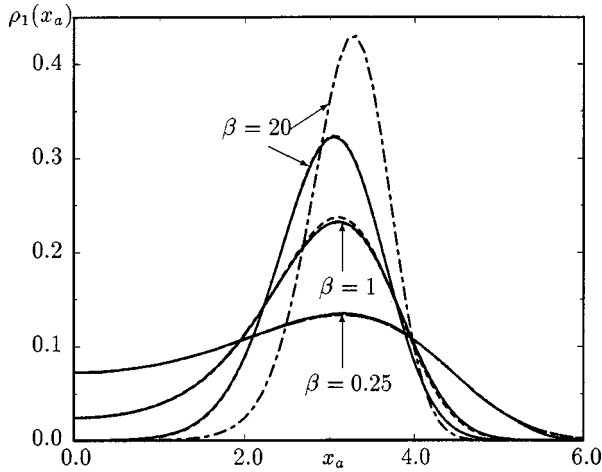


FIG. 9. First-order particle densities of the double well for $g = 0.1$ obtained by optimizing with respect to two variational parameters Ω^2 and x_m (dashed curves), and with only Ω^2 (dash-dotted line) vs exact distributions (solid) for different temperatures. The parameter x_m is very important for low temperatures.

$$\begin{aligned} & \int_0^\infty dx x^{\alpha-1} e^{-cx} L_m^\gamma(cx) L_n^\lambda(cx) \\ &= \frac{(1+\gamma)_m (\lambda-\alpha+1)_n \Gamma(\alpha)}{m! n! c^\alpha} \\ & \quad \times {}_3F_2(-m, \alpha, \alpha-\lambda; \gamma+1, \alpha-\lambda-n; 1), \end{aligned} \quad (8.24)$$

where $(\alpha)_n$ are Pochhammer symbols, ${}_pF_q(a_1, \dots, a_p; b_1, \dots, b_q; x)$ denotes the confluent hypergeometric function, and $\Gamma(x)$ is the gamma function, we apply the smearing formula to the interaction potential (8.19), and find

$$\begin{aligned} \langle \mathcal{A}_{\text{int}}[\mathbf{r}] \rangle_{\mathbf{r}_a, \mathbf{r}_a}^\Omega &= -\frac{e^2}{\sqrt{\pi} r_a} \sum_{n=0}^\infty \frac{(-1)^n (2n-1)!!}{2^n (2n+1)!} \\ & \quad \times C_\beta^{(2n)} H_{2n+1}(r_a / \sqrt{2a_{00}^2}) \\ & \quad - \frac{3}{4} \sqrt{2a_{00}^6} \Omega^4 \frac{1}{r_a} \left\{ C_\beta^{(0)} H_1(r_a / \sqrt{2a_{00}^2}) \right. \\ & \quad \left. + \frac{1}{6} C_\beta^{(2)} H_3(r_a / \sqrt{2a_{00}^2}) \right\}. \end{aligned} \quad (8.25)$$

The first term comes from the Coulomb potential, the second from the harmonic potential. Inserting Eq. (8.25) into Eq. (4.9), we compute the first-order isotropic form of the radial distribution function

$$g(\mathbf{r}) = \sqrt{2\pi\beta^3} \tilde{\rho}(\mathbf{r}). \quad (8.26)$$

This can be written as

$$g_1^\Omega(\mathbf{r}_a) = \exp[-\beta W_1^\Omega(\mathbf{r}_a)] \quad (8.27)$$

with the isotropic first-order approximation of the effective classical potential,

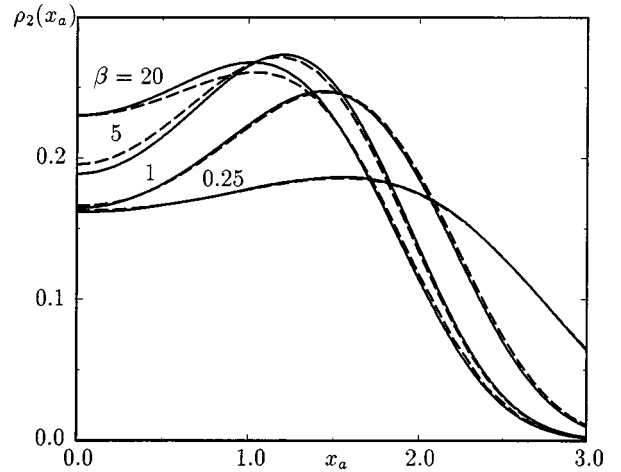


FIG. 10. Second-order particle density (dashed) compared with exact results from numerical solutions of the Schrödinger equation (solid) in a double well at different inverse temperatures. The coupling strength is $g = 0.4$.

$$W_1^\Omega(\mathbf{r}_a) = \frac{3}{2\beta} \ln \frac{\sinh \beta\Omega}{\beta\Omega} + \frac{\Omega}{\beta} r_a^2 \tanh \frac{\beta\Omega}{2} + \frac{1}{\beta} \langle \mathcal{A}_{\text{int}}[\mathbf{r}] \rangle_{\mathbf{r}_a, \mathbf{r}_a}^\Omega, \quad (8.28)$$

which is shown in Fig. 11 for various temperatures. The results compare well with Storer's precise numerical results [17]. Near the origin, our results are better than those obtained with an earlier approximation derived from the lowest-order effective classical potential given in Ref. [9].

2. Anisotropic first-order approximation

The above results can be improved by taking care of the anisotropy of the problem. For the harmonic part of action (8.18),

$$\mathcal{A}_{\text{int}}[\mathbf{r}] = \mathcal{A}^\Omega[\mathbf{r}] + \mathcal{A}_C[\mathbf{r}], \quad (8.29)$$

the smearing formula (7.7) yields the expectation value

$$\begin{aligned} \langle \mathcal{A}^\Omega[\mathbf{r}] \rangle_{\mathbf{r}_a, \mathbf{r}_a}^{\Omega, L, T} &= -\frac{1}{2} \{ \Omega_L^2 a_{L00}^2 (C_\beta^{(0)} + \frac{1}{2} C_{\beta, L}^{(2)} H_2(r_a / \sqrt{2a_{L00}^2})) \\ & \quad + 2\Omega_T^2 a_{T00}^2 (C_\beta^{(0)} - C_{\beta, T}^{(2)}) \}, \end{aligned} \quad (8.30)$$

where the $C_{\beta, L(T)}^{(n)}$ are the polynomials (6.5) with Ω replaced by the longitudinal or transverse frequency. For the Coulomb part of action (8.18), the smearing formula (7.7) leads to a double integral

$$\begin{aligned} \langle \mathcal{A}_C[\mathbf{r}] \rangle_{\mathbf{r}_a, \mathbf{r}_a}^{\Omega, L, T} &= -e^2 \int_0^{\hbar\beta} d\tau_1 \left(\frac{2}{\pi a_{L00}^2 (1-a_L^4)} \right)^{1/2} \\ & \quad \times \int_0^1 d\lambda \left\{ 1 + \lambda^2 \left[\frac{a_{T00}^2 (1-a_T^4)}{a_{L00}^2 (1-a_L^4)} - 1 \right] \right\}^{-1} \\ & \quad \times \exp \left\{ -\frac{r_a^2 a_L^4 \lambda^2}{2a_{L00}^2 (1-a_L^4)} \right\}, \end{aligned} \quad (8.31)$$

with the abbreviations

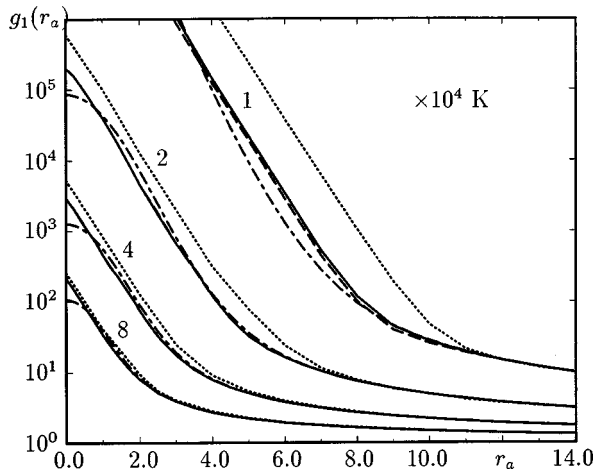


FIG. 11. Radial distribution function for an electron-proton pair. The first-order results obtained with isotropic (dashed curves) and anisotropic (solid line) variational perturbation theory are compared with Storer's numerical results [17] (dotted line) and an earlier approximation derived from the variational effective classical potential method to first order in Ref. [9] (dash-dotted line).

$$a_L^2 = \frac{a_{L00}^2}{a_{L01}^2}, \quad a_T^2 = \frac{a_{T00}^2}{a_{T01}^2}. \quad (8.32)$$

The integrals must be done numerically and the first-order approximation of the radial distribution function can be expressed by

$$g_1^{\Omega_L, T}(\mathbf{r}_a) = \exp[-\beta W_1^{\Omega_L, T}(\mathbf{r}_a)], \quad (8.33)$$

with

$$W_1^{\Omega_L, T}(\mathbf{r}_a) = \frac{1}{2\beta} \ln \frac{\sinh \beta \Omega_L}{\beta \Omega_L} + \frac{1}{\beta} \ln \frac{\sinh \beta \Omega_T}{\beta \Omega_T} + \frac{\Omega_L}{\beta} r_a^2 \tanh \frac{\beta \Omega_L}{2} + \frac{1}{\beta} \langle \mathcal{A}_{\text{int}}[\mathbf{r}] \rangle_{\mathbf{r}_a, \mathbf{r}_a}^{\Omega_L, T}. \quad (8.34)$$

This is optimized in $\Omega_L(\mathbf{r}_a), \Omega_T(\mathbf{r}_a)$, with the results shown in Fig. 11. The anisotropic approach improves the isotropic result for temperatures below 10^4 K.

IX. SUMMARY

We have presented variational perturbation theory for density matrices. A generalized smearing formula which accounts for the effects of thermal and quantum fluctuations was essential for the treatment of nonpolynomial interactions. We applied the theory to calculate the particle density in the double-well potential, and the electron density in the Coulomb potential, the latter as an example of nonpolynomial application. In both cases, the approximations were satisfactory.

ACKNOWLEDGMENT

The work of one of us (M.B.) is supported by the Studienstiftung des deutschen Volkes.

-
- [1] H. Kleinert, Phys. Lett. A **173**, 332 (1993).
 [2] H. Kleinert, *Path Integrals in Quantum Mechanics, Statistics and Polymer Physics*, 2nd ed. (World Scientific, Singapore, 1995).
 [3] W. Janke and H. Kleinert, Phys. Rev. Lett. **75**, 2787 (1995); Phys. Lett. A **206**, 283 (1995); R. Guida, K. Konishi, and H. Suzuki, Ann. Phys. (N.Y.) **249**, 109 (1996).
 [4] H. Kleinert, Phys. Rev. D **57**, 2264 (1998).
 [5] H. Kleinert, Phys. Lett. B **434**, 74 (1998).
 [6] H. Kleinert and H. Meyer, Phys. Lett. A **184**, 319 (1994).
 [7] H. Kleinert, W. Kürzinger, and A. Pelster, J. Phys. A **31**, 8307 (1998).
 [8] H. Kleinert, Phys. Lett. A **118**, 267 (1986).
 [9] W. Janke and H. Kleinert, Phys. Lett. A **118**, 371 (1986).
 [10] G. C. Rossi and M. Testa, Ann. Phys. (N.Y.) **148**, 144 (1983).
 [11] T. Kunihiro, Phys. Rev. Lett. **78**, 3229 (1997).
 [12] A. Coccoli, V. Tognetti, P. Verrucchi, and R. Vaia, Phys. Rev. A **45**, 8418 (1992). Also see the treatment of dissipation in A. Cuccoli, A. Rossi, V. Tognetti, and R. Vaia, Phys. Rev. E **55**, 4849 (1997).
 [13] R. Jackiw, Physica A **159**, 269 (1989).
 [14] A. Okopińska, Phys. Lett. A **249**, 259 (1998).
 [15] This quantity should not be confused with the standard *effective potential* in quantum field theory, in which the path average x_0 is not separated out. The effective classical potential always leads to a *convex* effective potential, due to the extra x_0 integral in Z. See H. Kleinert, Phys. Lett. B **181**, 324 (1986).
 [16] A. P. Prudnikov, Yu. A. Brychkov, and O. I. Marichev, *Integrals and Series* (Gordon and Breach, London, 1986), Vol. 2.
 [17] R. G. Storer, J. Math. Phys. **9**, 964 (1968).